Improved localization of implanted subdural electrode contacts on magnetic resonance imaging with an elastic image fusion algorithm in an invasive electroencephalography recording

Stieglitz, L H ; Ayer, C ; Schindler, K ; Oertel, M F ; Wiest, R ; Pollo, Claudio

Abstract: BACKGROUND: Accurate projection of implanted subdural electrode contacts in presurgical evaluation of pharmacoresistant epilepsy cases by invasive electroencephalography is highly relevant. Linear fusion of computed tomography and magnetic resonance images may display the contacts in the wrong position as a result of brain shift effects. OBJECTIVE: A retrospective study in 5 patients with pharmacoresistant epilepsy was performed to evaluate whether an elastic image fusion algorithm can provide a more accurate projection of the electrode contacts on the preimplantation magnetic resonance images compared with linear fusion. METHODS: An automated elastic image fusion algorithm (AEF), a guided elastic image fusion algorithm (GEF), and a standard linear fusion algorithm were used on preoperative magnetic resonance images and postimplantation computed tomography scans. Vertical correction of virtual contact positions, total virtual contact shift, corrections of midline shift, and brain shifts caused by pneumocephalus were measured. RESULTS: Both AEF and GEF worked well with all 5 cases. An average midline shift of 1.7 mm (SD, 1.25 mm) was corrected to 0.4 mm (SD, 0.8 mm) after AEF and to 0.0 mm (SD, 0 mm) after GEF. Median virtual distances between contacts and cortical surface were corrected by a significant amount, from 2.3 mm after linear fusion algorithm to 0.0 mm after AEF and GEF ($P < .001$). Mean total relative corrections of 3.1 mm (SD, 1.85 mm) after AEF and 3.0 mm (SD, 1.77 mm) after GEF were achieved. The tested version of GEF did not achieve a satisfying virtual correction of pneumocephalus. CONCLUSION: The technique provided a clear improvement in fusion of preimplantation and postimplantation scans, although the accuracy is difficult to evaluate.

DOI: https://doi.org/10.1227/NEU.0000000000000473

Originally published at:
Stieglitz, L H; Ayer, C; Schindler, K; Oertel, M F; Wiest, R; Pollo, Claudio (2014). Improved localization of implanted subdural electrode contacts on magnetic resonance imaging with an elastic image fusion algorithm in an invasive electroencephalography recording. Neurosurgery, 10(4):506-512.
DOI: https://doi.org/10.1227/NEU.0000000000000473

Improved Localization of Implanted Subdural Electrode Contacts on Magnetic Resonance Imaging With an Elastic Image Fusion Algorithm in an Invasive Electroencephalography Recording

Lennart Henning Stieglitz, MD*

Christian Ayer, MD‡

Kaspar Schindler, MD§

Markus Florian Oertel, MD¶

Roland Wiest, MD||

Claudio Pollo, MD¶

*Department of Neurosurgery, Zurich University Hospital, University of Zurich, Zurich, Switzerland; ‡University of Bern, Bern, Switzerland; §Department of Neurology, ¶Department of Neurosurgery, and ||Diagnostic and Interventional Neuroradiology, Inselspital, Bern University Hospital and University of Bern, Bern, Switzerland

Correspondence:
Lennart Henning Stieglitz, MD,
Department of Neurosurgery,
Zurich University Hospital,
8091 Zurich, Switzerland.
E-mail: lennart.stieglitz@usz.ch

Received, November 14, 2013.
Accepted, June 6, 2014.
Published Online, June 23, 2014.

BACKGROUND: Accurate projection of implanted subdural electrode contacts in presurgical evaluation of pharmacoresistant epilepsy cases by invasive electroencephalography is highly relevant. Linear fusion of computed tomography and magnetic resonance images may display the contacts in the wrong position as a result of brain shift effects.

OBJECTIVE: A retrospective study in 5 patients with pharmacoresistant epilepsy was performed to evaluate whether an elastic image fusion algorithm can provide a more accurate projection of the electrode contacts on the preimplantation magnetic resonance images compared with linear fusion.

METHODS: An automated elastic image fusion algorithm (AEF), a guided elastic image fusion algorithm (GEF), and a standard linear fusion algorithm were used on preoperative magnetic resonance images and postimplantation computed tomography scans. Vertical correction of virtual contact positions, total virtual contact shift, corrections of midline shift, and brain shifts caused by pneumocephalus were measured.

RESULTS: Both AEF and GEF worked well with all 5 cases. An average midline shift of 1.7 mm (SD, 1.25 mm) was corrected to 0.4 mm (SD, 0.8 mm) after AEF and to 0.0 mm (SD, 0 mm) after GEF. Median virtual distances between contacts and cortical surface were corrected by a significant amount, from 2.3 mm after linear fusion algorithm to 0.0 mm after AEF and GEF ($P < .001$). Mean total relative corrections of 3.1 mm (SD, 1.85 mm) after AEF and 3.0 mm (SD, 1.77 mm) after GEF were achieved. The tested version of GEF did not achieve a satisfying virtual correction of pneumocephalus.

CONCLUSION: The technique provided a clear improvement in fusion of preimplantation and postimplantation scans, although the accuracy is difficult to evaluate.

KEY WORDS: EEG, Elastic image fusion, Epilepsy, Invasive recording

Operative Neurosurgery 10:506–513, 2014 DOI: 10.1227/NEU.0000000000000473

In pharmacoresistant epilepsy cases, performing invasive investigation with intracranial electroencephalography (EEG) electrodes to localize the epileptogenic locus is often one of the last diagnostic options. In such cases, patients and physicians are driven by the hope of identifying a region of the brain where a resection might lead to significantly improved seizure control or even complete seizure freedom and increased quality of life. There are currently several accepted surgical methods to place electrode contacts on the brain surface to identify such regions.

ABBREVIATIONS: AEF, automated elastic fusion; **EEG,** electroencephalography; **GEF,** guided elastic fusion

The first method involves performing an extensive craniotomy and positioning a multicontact grid on the cortex.[1] The second but less invasive method involves stereotactic implantation of multiple electrodes inside the brain through a series of trepanations called stereo-EEG.[2,3] The third and least invasive method is the implantation of 4- to 10-contact strip electrodes on the cortex through a small number (at least 1 per side) of limited trepanations.[4] After electrode implantation, the direct positioning of the contacts on the cortex allows EEG recording with excellent signal-to-noise ratios and minimal muscle artifacts over several days and leads to a much better delineation of the epileptogenic zone compared with extracranially recorded EEG.[5] These EEG data can then be used for planning a potentially curative resective surgery, with the aim of achieving freedom from seizures.

All techniques enable exact localization of the contact position on the cortex, which is crucial for interpretation of the EEG signals. However, an imaging technology that allows visualization of metal electrode contacts and brain tissue simultaneously would be preferable. Unfortunately, magnetic resonance images (MRIs) can cause tissue damage as a result of energy transfer into heat.[5] Furthermore, the contacts cause artifacts in most imaging sequences that are far more intensive than the signal of the contacts themselves. On the other hand, in a computed tomography (CT) scan, the contacts can be visualized easily and even without image distortion, but because of artifacts around the contacts and the inferior quality of soft-tissue contrast, localization of the contacts in relation to the brain surface is also difficult.[6] The combination of both techniques using image fusion of preoperatively acquired MRI with post-operative CT scans is common and provides the required spatial information but is susceptible to the effects of brain shift. Cerebrospinal fluid (CSF) loss during electrode implantation and air trapped subdurally may cause a considerable dislocation of cortical structures.[7,8] A linear image fusion, allowing only translations, rotations, scaling, and skewness to align 2 image data sets, might localize the contacts in the wrong position.[9,10] Elastic image fusion algorithms are a relatively new development and are not yet standard in the commercial software used in neurosurgery. In addition to linear translations, they allow local modifications of the image data sets to achieve a better alignment. They may be helpful for solving this problem because theoretically they can compensate for these brain shift effects and enable visualization of the actual contact positions on the gyri. To analyze the preliminary results of such an innovative approach, a retrospective study in 5 patients with pharmacoresistant epilepsy was performed to evaluate whether an elastic image fusion algorithm can provide a more accurate projection of the electrode contacts on the preimplantation MRI than simple elastic fusion.

METHODS

Patients

Twenty-three patients (6 male and 17 female patients) suffering from pharmacoresistant epilepsy underwent an invasive recording phase between January and December 2011 at the Bern University Hospital (Inselspital). All patients had previously undergone a noninvasive recording phase, but the epileptogenic brain areas could not be localized as precisely as required to proceed directly to resective surgery.

Application of the elastic image fusion required a complete imaging data set, which is described in detail below. A subgroup of 5 patients, 2 male and 3 female patients with an average age of 19 years (SD, 2.9 years), ultimately fulfilled these requirements.

Preoperative and Postoperative Neuroimaging

For the stereotactic implantation of additional hippocampal depth electrodes,[11] all patients received preoperative and postoperative CT scans. Preoperatively, the patients underwent a T2 MRI scan (T2-weighted spin echo sequence: repetition time = 2200 milliseconds, slice thickness = 1 mm (gap, 0 mm), field of view = 256 mm, matrix = 256 × 256 on a 3-T Magnetom Verio MR system, Siemens Healthcare, Erlangen, Germany) and a native CT scan (tube current = 180 mA, kvp = 120 kV, standard kernel, slice thickness = 1 mm (supratentorial/infratentorial), and field of view = 220 mm on a GE Lightspeed 8-row detector scanner, GE Healthcare, Milwaukee, Wisconsin). Postoperatively (day of surgery), all patients received an additional native CT scan as described above.

Electrode Implantation Technique

To reduce morbidity and to allow maximal coverage of the brain surface, we implanted multiple 4- to 6-contact strip electrodes in a star-like manner from frontal and frontotemporal regions via 14-mm trepanations. To minimize the risk of infection, the patient's head was shaved and intravenous antibiotics were given perioperatively. The ideal positions of the trepanations were localized with the use of a neuronavigation system (VectorVision2, BrainLab, Feldkirchen, Germany). Under general anesthesia, trepanation was performed and the dura was opened. Four- to 8-contact strip electrodes (Ad-Tech medical Instrument Corporation, Racine, Wisconsin) were implanted under neuronavigation and fluoroscopic guidance (Table 1). Depending on the clinical presentation of the patient, 1 burr hole was placed unilaterally or bilaterally over the sylvian fissure with 3 to 4 strips going around the temporal lobe and 2 to 4 strips covering the frontal and frontoparietal lobes. To reduce CSF loss, the trepanation was sealed with fibrin glue after implantation of the final electrode. The cables were subcutaneously tunneled and externalized through the skin at least 4 cm distant from the trepanation site to reduce infection. Postoperatively, the position of the electrode contacts and the absence of potential subdural hematomas were confirmed on a native CT scan.

Image Coregistration

The most common method used for coregistration of 2 image data sets is the so-called mutual information method. Originating from the information theory, this method measures the statistical dependency between 2 data sets and has been shown to perform well in coregistration of CT and MRI.[12,13] In linear coregistration, the alignment of the 2 data sets is achieved by translation, rotation, scaling, and skewness, each along 3 *df*, adding up to 12 *df* altogether. Elastic coregistration should be able to, in addition to the linear translation, apply changes only locally and thus deliver more precise results, especially when the image acquisition time is different or even when preoperative and postoperative data sets are to be fused.

Linear Image Fusion

All image fusions were performed with a prerelease version provided by Brainlab iPlan (Brainlab, Feldkirchen, Germany). The algorithm for linear image fusion applies 12 *df* and is identical to that included in the commercial software version iPlan 3.0. The region of interest is automatically defined and covers the entire skull of the patient. In all fusion procedures, the postoperative CT scan was fused onto the preoperative MRI scan.

Elastic Image Fusion

The elastic image fusion was performed using 2 different versions of the elastic fusion algorithm. The first, referred to as automated

TABLE 1. Electrode Contacts Implanted[a]

Patient	Laterality	Region	Contacts, n
1	Left	Temporopolar	6
		Posterior temporal	6
	Right	Temporopolar	6
		Anterior temporal	6
		Posterior temporal	6
2	Left	Temporopolar	4
		Anterior temporal	6
		Medial temporal	6
		Posterior temporal	6
	Right	Temporopolar	4
		Anterior temporal	6
		Medial temporal	6
		Posterior temporal	6
3	Left	Temporopolar	6
		Anterior temporal	6
		Medial temporal	6
		Posterior temporal	6
	Right	Temporopolar	6
		Anterior temporal	6
		Medial temporal	6
		Posterior temporal	6
4	Left	Temporopolar	6
		Anterior temporal	6
		Medial temporal	6
		Posterior temporal	6
		Inferior frontal	6
		Superior frontal	8
		Frontoparietal	8
		Parietal	8
	Right	Temporopolar	6
		Anterior temporal	6
		Medial temporal	6
		Posterior temporal	6
		Inferior frontal	6
		Superior frontal	8
		Frontoparietal	8
		Parietal	8
5	Left	Temporopolar	4
		Anterior temporal	6
		Medial temporal	6
		Posterior temporal	6
	Right	Temporopolar	4
		Anterior temporal	6
		Medial temporal	6
		Posterior temporal	6
Total contacts implanted, n			274

[a]The table shows the positions and numbers of contacts per electrode implanted in each patient.

elastic fusion (AEF), tries to find a corresponding position in the first data set for each structure in the second. The algorithm runs fully automated.

The second, referred to as guided elastic fusion (GEF), allows manual definition of corresponding structures in both images. During the automated fusion process, these manually defined structures may have no counterpart in the other data set. Examples for such structures are tumors in preoperative and postoperative images and intracranial air, which are not present in preoperative images. In the present study, we segmented intracranial air for GEF.

Both algorithms allow deformation of an underlying grid in 3 dimensions to achieve an optimal fit of the anatomic structures. Figure 1 shows a deformation map indicating the direction and intensity of deformation for each position of the grid. Just like in the linear fusion processes, the postoperative CT scans were elastically fused onto the preoperative MRI.

Assessment of the Effect of Elastic Image Fusion on Virtual Brain Shift

CSF loss and the resulting pneumocephalus often lead to a lateral shift of the midline to the contralateral side. Therefore, as the most straightforward parameter, the lateralization of the midline at the level of the foramen of Monroe was measured in millimeters after both linear and elastic image fusion using the 2 different software versions, AEF and GEF.

Second, the size of frontally trapped subdural air was judged in the postoperative CT after linear and after elastic image fusion. The maximum thickness in an axial slice and the volume of trapped air were measured.

After linear image fusion, the electrode contacts on CT are sometimes virtually projected inside the cortex or even subcortically. An optimal fusion should enable visualization of the electrode contacts correctly on the cortical surface and should compensate for brain shift effects. To examine the ability of both elastic fusion algorithms (AEF and GEF) to achieve this, we measured the distances of the positions of the virtual contacts and the brain surface and compared the results with the position of the contacts after linear image fusion. The distances, given in millimeters, are measured separately in the frontal, parietal, and temporal regions. Furthermore, the shortest distance between electrode contacts after linear and elastic image fusion was measured to judge the dimension of the effect of the elastic fusion.

Statistics and Ethics

All patient data were anonymized before import into the iPlan software. The local ethics committee approved this retrospective analysis. Statistical analyses included the Welch 2-sample *t* test and Wilcoxon nonparametric test using R statistics programming language.[14] A value of $P < .05$ was considered significant. All values were not normally distributed (Shapiro-Wilk normality test).

RESULTS

Midline Shift Correction

Correction of the midline shift was one of the major parameters used to evaluate the accuracy of the elastic fusion. As a point of reference, to measure this shift, we defined an axial slice through the septum pellucidum directly above the foramen of Monro. Although the median midline shift in the postoperative CT (evaluated by linear image fusion) was 1.9 mm, it was corrected to a median of 0 mm by both AEF and GEF. Because of the small number of patients included in the study, the result was not statistically significant (Table 2).

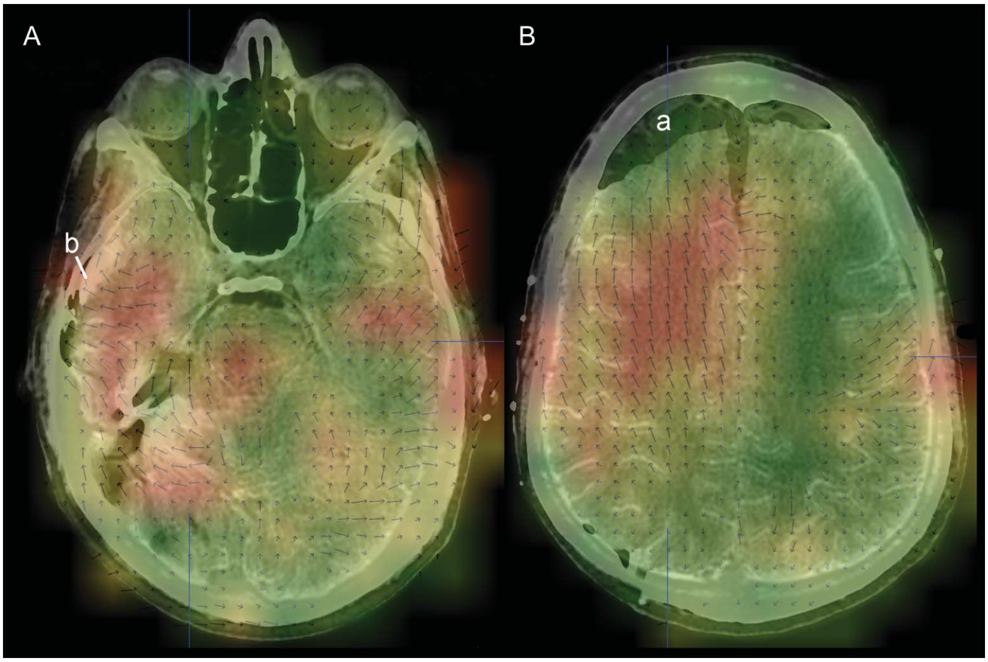

FIGURE 1. *Three-dimensional deformation map of elastic image fusion between a magnetic resonance image and a computed tomography. Green shows areas of minor deformation; red, areas with strong deformation.* **A**, *axial section at the level of the temporal lobes. The artifact of subdurally implanted electrode contacts is shown (b).* **B**, *axial section at the level of the frontal lobes. A relevant right frontal pneumocephalus and its effect on the brain tissue are shown (a).*

Pneumocephalus Correction

The second task for elastic fusion algorithms was the correction of pneumocephalus in the fused images. Neither AEF nor GEF corrected sufficiently for this problem, as shown for measurements of frontal air thickness (Table 3) and air volumetry (Table 4). Therefore, the elastic fusion algorithms used in the present study ultimately provided no significant reduction of pneumocephalus.

Electrode Contact Position

Both AEF and GEF achieved an effective reduction of the electrode-cortex distance, as shown in Figure 2. This result was achieved in all tested areas: frontal, temporal, and parietal regions. The reduction of distance compared with the linear fusion was statistically significant (Wilcoxon, $P < .001$; Table 5).

Relative Virtual Electrode Contact Position Correction

Elastic image fusion led to relevant virtual shifts of the electrode contact positions by median distances of 2.9 mm (AEF) and 2.8 mm (GEF) (Table 5). Differences between the 2 fusion algorithms tested in this study were not statistically significant. However, statistically significant regional differences were found for the frontal vs temporal cortices ($P = .03$) and the frontal vs parietal cortices ($P < .001$).

TABLE 2. Midline Shift Correction[a]

	No Correction	AEF	GEF
Median (mm)	1.90	0	0
IQR	0.75	0.4	0
P		.14 (RF/AEF)	.07 (RF/GEF)
P		.39 (AEF/GEF)	

[a]AEF, automated elastic fusion; GEF, guided elastic fusion; RF, rigid fusion. The table shows the midline shift measured at the septum pellucidum after AEF and GEF, and the results compared with the uncorrected computed tomography.

TABLE 3. Reduction of Frontal Pneumocephalus Measured as Cortex-Bone Distance[a]

	No Correction	AEF
Median	9.8	9.2
IQR	5.2	4.88
P		.68

[a]AEF, automated elastic fusion. The table shows the maximum thickness of frontal intracranial air measured in an axial slice. The AEF did not lead to a sufficient correction of the brain shift effect.

TABLE 4. Volumetric Reduction of Frontal Pneumocephalus[a]	No Correction	Elastic Fusion
Median, mm	19.49	19.1
Interquartile range, mm	20.7	17.18
P		.86

[a]As a measurement of the thickness of the pneumocephalus, the volumetric measurement does not show a satisfying correction of the brain shift effect.

DISCUSSION

Invasive recording workup for patients suffering from pharmacoresistant epilepsy is often a stressful and demanding procedure for both the patient and the attending physician. Although the procedure can be considered safe, effective, and a gold standard, implantation of electrodes into the skull and brain exclusively for diagnostic purposes is an option that only patients desperate for treatment of their seizures will undergo. This makes it especially important that everything is done to make the results optimally useful for treatment planning. Accurate projection of the implanted electrode contacts on the brain surface is a crucial step, especially when it involves resection planning in or close to eloquent cortex. With grid implantation through craniotomy, the brain surface can be photographed and images can be superimposed onto a cortical MRI reconstruction.[15-20] Combinations of photography and 2-dimensional radiography have been described,[10] as have linear superpositions using a 3-dimensional visualization system.[9] Contacts under the margins of the craniotomy or placed through burr holes cannot be documented photographically; these contacts are also subject to brain shift, which can be corrected mathematically.[7,20]

Using the anatomic information of the CT scan and combining this with the high spatial and contact soft-tissue resolution of MRI provide a potential new option to handle this situation. Modern computers allowing highly complex calculations, together with newly developed elastic fusion algorithms, can be used to compensate for brain shift effects in the future. The algorithms tested and presented here performed the fusion in 5 to 10 minutes per case on a BrainLab iPlan server (HP ProLiant DL360p Gen 8: 2xIntel Xeon E5-2667, 2.9 GHz, 32 GB RAM, 4 × 300 GB HDD). One possible use is the fusion of postoperative CT after subdural electrode implantation with preoperative MRI for contact superposition.

Display of Electrode Contacts on the Brain Surface

Linear fusion of preoperative and postoperative images often localizes the position of the electrode contacts incorrectly, often

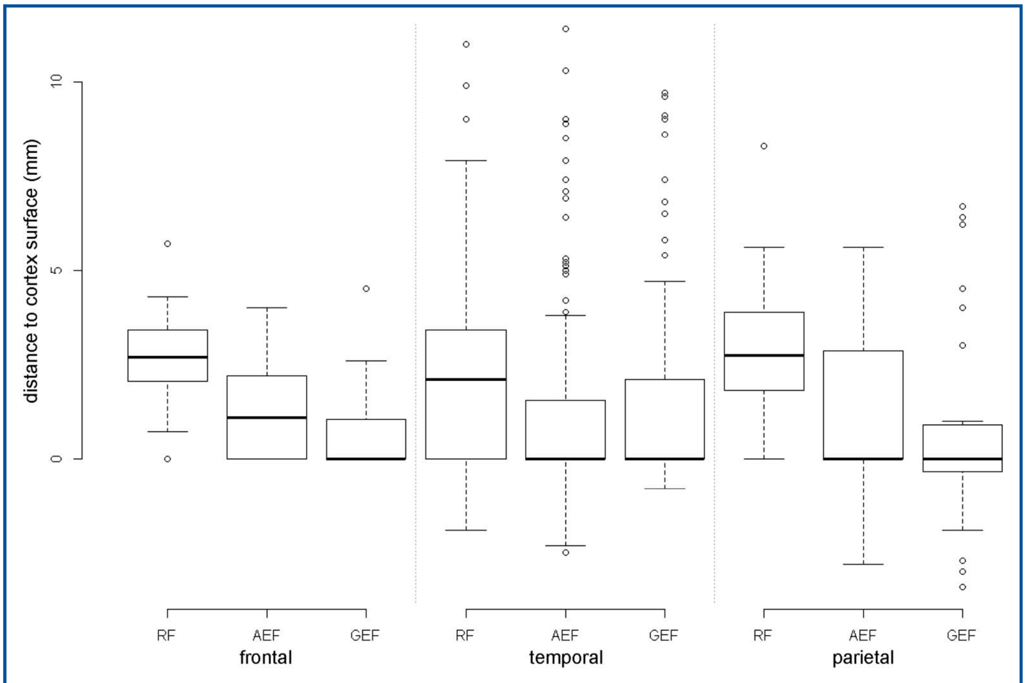

FIGURE 2. *Distance between the electrode contact center and cortex surface. The figure shows a highly effective reduction of the distance between the electrode contact centers and the cortical surface, from a median of 2.3 to 0 mm after automated elastic fusion (AEF) and guided elastic fusion (GEF) in the frontal region compared to rigid fusion (RF). Reductions were also measured in the temporal and parietal regions. All reductions are significant (GEF in temporal region,* P *= .03; all others,* P *< .001). Thick lines indicate medians; boxes, the interquartile range; and whiskers, ±1.58 × the interquartile range. Outliers are shown as open circles.*

TABLE 5. Relative Correction of Electrode Contact Position by Elastic Fusion[a]

	All		Frontal		Temporal		Parietal	
Region	**AEF**	**GEF**	**AEF**	**GEF**	**AEF**	**GEF**	**AEF**	**GEF**
Median	2.9	2.8	2.45	2.45	2.8	2.6	4.3	4.5
Interquartile range	2.53	2.5	2.1	1.88	2.53	2.45	1.8	2.45
P	.55		.99		.42		.96	
			[.03]					
					<.001			
			<.001					

[a]AEF, automated elastic fusion; GEF, guided elastic fusion. Elastic fusion led to localization of the electrode contacts relative to their original positions in the postoperative computed tomography. AEF and GEF achieved nearly identical shifts in all regions. The shift was significantly higher in the temporal than in the frontal region and was greatest in the parietal region.

inside the cortex or even subcortically (Figure 3A and 3C). AEF led to a display of the contacts that was clearly distant from where they were shown after linear fusion. The effect was stronger in the temporal than in the frontal region and impacted contacts implanted parietally. Some of the subgroups of contacts in different brain regions are very small and allow only limited interpretation.

After elastic fusion (both AEF and GEF), the contacts displayed were clearly closer to the brain surface (Figure 3B and 3D). However, a clear superiority of the GEF over the AEF could not be shown.

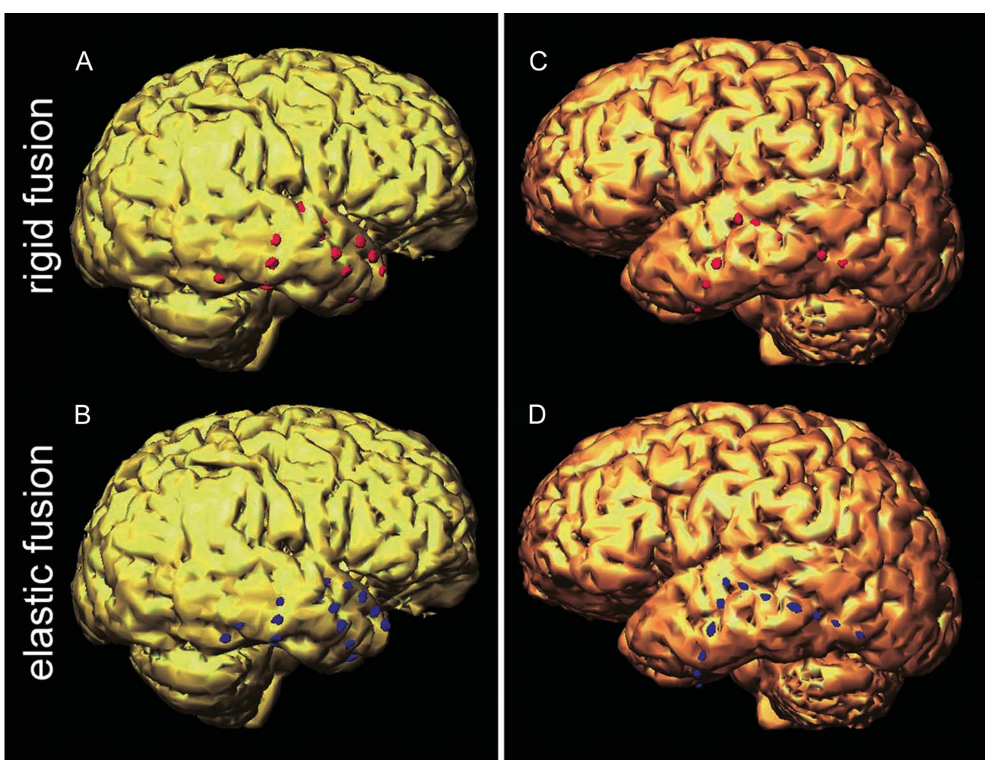

FIGURE 3. *Projection of electrode contacts on the brain surface after linear and elastic image fusion. The figure shows the temporal electrode contacts of 2 illustrative cases after linear (**A** and **C**) and elastic (**B** and **D**) fusion. After linear fusion, some of the contacts are virtually buried in the tissue. Elastic fusion provides a more plausible projection of the contacts onto the brain surface.*

Plausibility of the Results

Because there are usually few landmarks visible on both CT and MRI to evaluate the quality of the elastic fusion, correction of major shift effects was used to validate the fusion results. The interhemispheric midline should normally be located in the middle of the skull. However, shifts to either side can occur after trepanation of the skull, loss of CSF, intracranial trapping of air, brain swelling, or resection of space-occupying lesions or epileptogenic brain tissue. Both elastic fusion algorithms completely compensated for the midline shift.

Originally, our purpose was to develop a simple automated fusion algorithm. Unfortunately, the elastic fusion algorithms were not accurate enough to compensate for the shift caused by pneumocephalus. The finding that this algorithm did not sufficiently deal with additional volumes or nonexistent volumes in either of the fused images led to the idea of creating an additional guided algorithm. The GEF has the advantage that it uses corresponding points or structures in both image sets to support the automated structure detection. Furthermore, a function was added to define a volume in one of the image sets that might undergo major change or might not be present in the other image set. Potential examples therefore might be a tumor removed, a hematoma evacuated, or intracranial air inoculated.

Validation of elastic image fusion results is very difficult in cases in which there is no way to document the electrode contact positions visually. A photographic documentation of the electrode contact positions would have been preferable, as shown by Tao et al,[17] LaViolette et al,[18] and Pieters et al,[19] in cases in which a grid was implanted through a craniotomy. Dykstra et al[20] faced the same problem we do with localizing electrode contacts that are implanted through burr holes. Not being able to compare with intraoperative photographs, they simply shift the electrode contacts to the level of the pia.

CONCLUSION

We demonstrated that elastic fusion can produce more plausible results than linear fusion, but the available algorithms must be developed further to deal with complex situations such as fusing preoperative and postoperative images.

The technique is fast and fully automated and offers high flexibility. The scope of possible applications of the presented software is not limited to epilepsy surgery. Another possible field of application is fusion of preoperative and postoperative images after tumor resection to better identify the position of tumor remnants in the preoperative MRI.

Further Software Development

We thank BrainLab, Germany for kindly providing the 2 elastic fusion algorithms used in this study. The software applied in the present study is constantly refined. The results presented here do not necessarily represent the abilities of the most recent software version; experiences and results driven by our work directly influenced the further development of the software.

Disclosure

The authors have no competing interests. No specific funding was provided for this project. The providers of the software tested had no role in the study design, data collection, data analysis, decision to publish, or preparation of the manuscript. The authors have no personal, financial, or institutional interest in any of the drugs, materials, or devices described in this article.

REFERENCES

1. Vadera S, Mullin J, Bulacio J, Najm I, Bingaman W, Gonzalez-Martinez J. Stereoelectroencephalography following subdural grid placement for difficult to localize epilepsy. *Neurosurgery*. 2013;72(5):723-729; discussion 729.
2. Gonzalez-Martinez J, Mullin J, Vadera S, et al. Stereotactic placement of depth electrodes in medically intractable epilepsy. *J Neurosurg*. 2014;20(3):639-644.
3. Bancaud J, Talairach J. *La Stéréo-ÉlectroEncéphaloGraphie dans l'épilepsie*. Paris, France: Masson & Cie; 1965:35-122.
4. Wyler AR, Ojemann GA, Lettich E, Ward AA. Subdural strip electrodes for localizing epileptogenic foci. *J Neurosurg*. 1984;60(6):1195-1200.
5. Bhavaraju NC, Nagaraddi V, Chetlapalli SR, Osorio I. Electrical and thermal behavior of non-ferrous noble metal electrodes exposed to MRI fields. *Magn Reson Imaging*. 2002;20(4):351-357.
6. Hastreiter P, Rezk-Salama C, Soza G, et al. Strategies for brain shift evaluation. *Med Image Anal*. 2004;8(4):447-464.
7. Hermes D, Miller KJ, Noordmans HJ, Vansteensel MJ, Ramsey NF. Automated electrocorticographic electrode localization on individually rendered brain surfaces. *J Neurosci Methods*. 2010;185(2):293-298.
8. Serra C, Huppertz H-J, Kockro RA, et al. Rapid and accurate anatomical localization of implanted subdural electrodes in a virtual reality environment. *J Neurol Surg a Cent Eur Neurosurg*. 2013;74(3):175-182.
9. Dalal SS, Edwards E, Kirsch HE, Barbaro NM, Knight RT, Nagarajan SS. Localization of neurosurgically implanted electrodes via photograph-MRI-radiograph coregistration. *J Neurosci Methods*. 2008;174(1):106-115.
10. Miyagi Y, Shima F, Sasaki T. Brain shift: an error factor during implantation of deep brain stimulation electrodes. *J Neurosurg*. 2007;107(5):989-997.
11. King D, Bronen RA, Spencer DD, Spencer SS. Topographic distribution of seizure onset and hippocampal atrophy: relationship between MRI and depth EEG. *Electroencephalogr Clin Neurophysiol*. 1997;103(6):692-697.
12. Pluim JPW, Maintz JBA, Viergever MA. Mutual-information-based registration of medical images: a survey. *IEEE Trans Med Imaging*. 2003;22(8):986-1004.
13. Hill DL, Batchelor PG, Holden M, Hawkes DJ. Medical image registration. *Phys Med Biol*. 2001;46(3):R1-R45.
14. R Development Core Team. *R: A Language and Environment for Statistical Computing*. Vienna, Austria; 2008. http://www.r-project.org. Accessed May 14, 2013.
15. Wellmer J, von Oertzen J, Schaller C, et al. Digital photography and 3D MRI-based multimodal imaging for individualized planning of resective neocortical epilepsy surgery. *Epilepsia*. 2002;43(12):1543-1550.
16. Mahvash M, König R, Wellmer J, Urbach H, Meyer B, Schaller K. Coregistration of digital photography of the human cortex and cranial magnetic resonance imaging for visualization of subdural electrodes in epilepsy surgery. *Neurosurgery*. 2007;61(5 suppl 2):340-344; discussion 344-345.
17. Tao JX, Hawes-Ebersole S, Baldwin M, Shah S, Erickson RK, Ebersole JS. The accuracy and reliability of 3D CT/MRI co-registration in planning epilepsy surgery. *Clin Neurophysiol*. 2009;120(4):748-753.
18. LaViolette PS, Rand SD, Ellingson BM, et al. 3D visualization of subdural electrode shift as measured at craniotomy reopening. *Epilepsy Res*. 2011;94(1-2):102-109.
19. Pieters TA, Conner CR, Tandon N. Recursive grid partitioning on a cortical surface model: an optimized technique for the localization of implanted subdural electrodes. *J Neurosurg*. 2013;118(5):1086-1097.
20. Dykstra AR, Chan AM, Quinn BT, et al. Individualized localization and cortical surface-based registration of intracranial electrodes. *Neuroimage*. 2012;59(4):3563-3570.

COMMENTS

This study reports a method of image nonlinear registration to localize the actual position of subdural electrodes (SDEs) on preoperative 3-dimensional magnetic resonance imaging (MRI). This issue is crucial because the direct localization of the implanted devices in the postoperative images is difficult and imprecise as a result of the metal artifacts on both MR and computed tomography (CT) scans. The registration of postimplantation CT scans to the preoperative MR is a commonly adopted method, but the linear approach does not account for the displacement of the intracranial structures occurring after SDE implantation, mainly because of brain shift secondary to cerebrospinal fluid leakage, pneumocephalus, pericerebral fluid collection, and the space-occupying effect of the array of electrodes. The authors rely on 2 slightly different techniques allowing the nonlinear registration of a postimplantation 3-dimensional CT scan to a 3-dimensional preoperative MRI. After registration with the nonlinear approaches, the median distance of the SDEs from the cortical surface of the preimplantation MRI approximates zero in the different brain regions explored, significantly improving the results obtained with standard rigid registration. The authors conclude that nonlinear registration provides more plausible results compared with rigid registration as to localization of actual position of SDEs. They also indicate possible future developments and applications of the described technique.

This study reports for the first time, as far as we know, the application of nonlinear registration to the localization of SDEs. The latter issue is essential for the appropriate interpretation of intracranial electroencephalography data (eg, correct topographic identification of a specific electrical activity and/or function) and consequently for adequate conduction of surgical resections in epilepsy surgery cases. In fact, incorrect localization of SDE may result in incorrect localization of the epileptogenic zone and of eloquent cortical areas, with potentially deleterious effects on seizure and functional outcome. In this context, the proposed technique has promising and interesting potentials.

The main limit of this study, however, is the lack of verification of the accuracy of the obtained SDE–cortical surface topographic relationships by direct visual inspection because the positioned strips inserted through burr holes cannot be directly visualized. The described technique of SDE localization by nonlinear registration therefore requires further verification in patients receiving grid electrodes implanted via craniotomy. This would allow accuracy evaluation by 2-dimensional digital photography and would possibly provide additional strength to this localization methodology.

Nonlinear registration methods were developed many years ago, but they were not used for a long time because of their high complexity and computational load. Nowadays, given the high power of modern computers, they are gaining popularity in 3 main fields of neurosciences: the intrasubject registration of intraoperative images (CT and MR) and of preoperative and postoperative images and the intersubject registration for population studies. Although in the case of intraoperative registration the computational time is crucial, in the last 2 cases the adopted algorithms can be more complex to give even better results. The software tools described in this study are very fast because they were developed in the context of "real-time" devices for neuronavigation. In the future, it will be interesting to compare these optimized nonlinear approaches with some others that could give better results at the cost of increased computational time.

Massimo Cossu
Francesco Cardinale
Milan, Italy

The authors present a nonrigid deformation protocol for coregistration of 2 data sets that may have distortion with respect to one another such as is caused by subdural air, loss of cerebrospinal fluid, tumor resection, etc. After intracranial monitoring surgery in which several strip electrodes were inserted via burr hole trephination, the algorithm was shown to compensate for midline shift and electrode shift but not pneumocephalus. The result depicted surface electrodes detected on postoperative computed tomography as being apposed to the brain surface as detected on preoperative magnetic resonance imaging (MRI), whereas a linear coregistration (standard on navigational workstations) showed, for example, surface electrodes residing within the parenchyma. This is a useful approach and will help in depicting the location of surface invasive monitoring electrodes in a more realistic fashion. This will facilitate showing the relationship of the electrodes to both structural features (eg, tumors, dysplasias) and functional features (eg, regions of activation on functional MRI, positron emission tomography hypometabolism, single-photon emission computed tomography activation), which helps in interpreting monitoring data and planning mapping and resections. We have also used a nonrigid deformation algorithm to quantify brain shift.[1] The algorithm used here was not sufficiently robust to compensate for (ie, "eliminate") pneumocephalus, possibly because of the small local field used. The necessity for such algorithms results from no ideal postoperative imaging modality that both depicts electrodes with minimal artifact and the brain anatomy. The argument that postimplantation MRI cannot be used for safety regions is specious: we (and others) routinely obtain volumetric MRI studies postoperatively without encountering a single adverse effect. The electrode artifact is indeed more difficult to contend with. Perhaps the advent of more MRI-compatible electrodes in the future will mitigate this problem and render coregistration algorithms moot for structural analyses. Nevertheless, the problem of coregistration to preoperative functional studies remains, and the present nonrigid deformation may become a useful tool in the near future for the practice of epilepsy surgery.

Robert E. Gross
Atlanta, Georgia

1. Khan MF, Mewes K, Gross RE, Skrinjar O. Assessment of brain shift related to deep brain stimulation surgery. *Stereotact Funct Neurosurg.* 2008;86(1):44-53.